 SID, vol.1, no.1, pp.35-47, 2005

2D Wave Scattering by a Crack in a Piezoelectric Plane Using Traction BIEM

D. Gross[1] **, T. Rangelov** [2] **, and P. Dineva** [3]

Abstract: Scattering of time harmonic waves by a finite crack in a homogeneous piezoelectric plane under plane strain conditions is studied. Using generalized displacements and tractions, the problem is described by a non-hypersingular traction based boundary integral equation method (BIEM). The fundamental solution is derived in closed form by Radon transforms. As a typical example, the procedure is applied to a straight crack under incident longitudinal waves and under vertically polarized shear waves. The K-factor results are compared with those from the literature for a special case. Furthermore, their dependence on parameters like frequency, angle of incidence, wave type and material properties is discussed.

keyword: Piezoelectric, materials, Wave scattering, BIEM, SIF.

1 Introduction

Piezoelectric ceramic materials are anisotropic dielectrics, where both the electric and the elastic fields are coupled. They are extensively utilized as transducers, sensors and actuators in many fields like telecommunication, robotics, microelectronics, mechatronic or adaptive intelligent structures. Piezoelectric materials are inherently brittle. The components made from them usually contain natural flaws due to the manufacturing process and unavoidable artificial stress concentrators on account of their specific composition e.g. as actuating component. This is the reason why linear fracture analysis plays an important role for analyzing the electro-mechanical behavior including reliable failure and lifetime predictions. The knowledge of electro-mechanical stress intensity factors (SIF) for static and dynamic loading conditions may provide useful information concerning crack initiation and final fracture of a structure.

The theoretical basis for the description of linear piezoelectrics can be found in Landau & Lifshitz (1960), Parton & Kudryavtsev (1988), Ikeda (1990) and Eringen & Maugin (1990). During the past decades, many papers on crack problems for such materials have been published which may be divided into the following groups. (A) Analytical solutions for simple crack geometries and loading conditions, see e.g. Parton (1976), Pak(1990), Sosa (1992), Xu & Rajapakse (1999). (B) Green's function approach and fundamental solution for static and dynamic problems that have a relatively simple mathematical structure and which are convenient for numerical implementation. As examples for time-harmonic 3D problems Norris (1994), Khutoriansky & Sosa (1995a,b), Sosa & Khutoriansky (1999, 2001) and for 3D problems in the time-domain Daros & Anthes (2000) shall be mentioned. A fundamental solution for transient 2D and 3D problems was derived by Daros (2002); fundamental solutions for 2D problems in the time-domain and frequency domain have been given by Gross, Dineva & Rangelov (2002), Wang, Zhang & Hirose (2003), Wang & Zhang (2004), Rangelov & Dineva (2004), Gross, Dineva & Rangelov (2004), Denda, Araki & Yong (2004). A fundamental solution for the 2D antiplane problem was derived by Wang & Meguid (2000b). (C) Development of approximate semi-analytical solution methods, see Shindo and Ozawa (1990), Shindo, Katsure & Yan (1996), Narita & Shindo (1998), Wang & Meguid (2000a), Wang & Noda (2000). (D) Development of numerical methods as the FEM, see Kumar & Singh (1997a,b), McMeeking (1999), Benjeddou (2000), Shang, Kuna & Abendroth (2003) and the BIEM, see Khutoryansky & Sosa (1995a), Chen & Lin (1995), Hill & Farris (1998), Pan (1999), Lee (1999), Denda & Lua (1999), Davi & Milazzo (2001).

Restricting the focus on time-harmonic solutions a few more investigations have to be mentioned. An analyti-

[1] Institute of Mechanics, Darmstadt University of Technology, 64289 Darmstadt, Germany.
[2] Institute of Mathematics and Informatics, Bulgarian Academy of Sciences, 1113 Sofia, Bulgaria.
[3] Institute of Mechanics, Bulgarian Academy of Sciences, 1113 Sofia, Bulgaria.

cal solution for a simply supported composite plate under harmonic electrical load was given by Ray, Bhattacharya & Samanta (1998). A closed form solution for the antiplane problem of a single crack in an infinite region based on the dual singular integral equations method was presented by Chen & Yu (1998) and Parton & Kudryavtsev (1988). Shindo & Ozawa (1990) first investigated the dynamic response of a cracked domain under normal incident in-plane longitudinal waves by using Fredholm integral equations. The diffraction of anti-plane shear waves with arbitrary angle of incidence by a crack in an infinite orthotropic piezoelectric ceramic has been investigated by Narita & Shindo (1998). The equivalent two-crack diffraction problem was solved by Wang & Meguid (2000a, b). Zhao & Meguid (2002) investigated the dynamic behavior of a piezoelectric laminate containing multiple interfacial collinear cracks subjected to electro-mechanical loads. Finally Saez, Dominguez & Garcia-Sanchez (2004) shall be mentioned who recently presented results for different crack geometries based on Green's function approach.

From this short review it can be concluded that the number of papers and results regarding wave diffraction by cracks in piezoelectric continua is still restricted. This fact may be explained by the complexity of the governing equations, the different possibilities of electrical boundary conditions and the mathematical difficulties of developing appropriate solution methods. A well developed solution method for wave diffraction problems is the method of dual singular integral equations and most of the cited results have been obtained by its usage. Because of its relative simplicity there exist more results for the anti-plane case and only a few for the in-plane case which is of higher practical interest. In contrast to conventional fracture mechanics there exist no dynamic in-plane BIEM formulation and results for piezoelectrics. The main reason for this is that the derivation and usage of the fundamental solutions for dynamic piezoelectricity is relatively complex due to the anisotropy and the electromechanical coupling.

Aims of this work are to present a time-harmonic fundamental solution in closed form, to develop a non-hypersingular, traction-based BIEM and to show its applicability. For this purpose, numerical results for the 2D in-plane wave diffraction problem in infinite cracked piezoelectric transversely isotropic planeregion are presented and discussed.

The paper is structured as follows. In section 2 the boundary value problem is described and its traction BIE formulation is given. The fundamental solution for the governing equations is derived by Radon transforms in section 3. Section 4 describes the numerical implementation. Finally, the validation of the BIEM solution and a series of numerical results for a finite crack subjected to L and SV-waves with different angles of incidence and for different material parameters are discussed in section 5, followed by a conclusion in section 6.

2 Problem statement and traction BIE

We consider an infinite homogeneous piezoelectric plane region containing an arbitrary shaped crack S_{cr}, see Figure 1. Using the coordinates x_1, x_3 and assuming plane

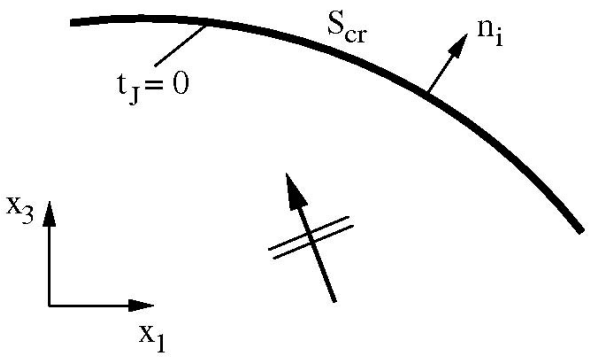

Figure 1 : Piezoelectric plane region with an arbitrary shaped crack.

strain conditions, the non-zero field quantities are the displacement u_i, the stresses σ_{ij}, the electric displacement D_i and the electric field intensity E_i, where $i, j = 1$ or 3. The basic equations of linear piezoelectricity in absence of body forces and charges consist of the balance equations

$$\sigma_{ij,j} = \rho \ddot{u}_i \quad D_{i,i} = 0 \tag{1}$$

and the kinematical and electric field-potential relations

$$s_{ij} = \frac{1}{2}(u_{i,j} + u_{j,i}) \quad E_i = -\phi_{,i} \tag{2}$$

where s_{ij}, Φ and ρ are the strain tensor, the electric potential and the mass density, respectively. The summation convention for repeated indices is implied, subscript

commas denote differentiation with respect to spatial coordinates while superscript dots indicate time derivatives. Introducing the generalized displacement $u_K = (u_1, u_3, \Phi)$, $J, K = 1,3$ or 4, the constitutive equations can be written as

$$\sigma_{iJ} = C_{iJKl} u_{K,l} = C_{iJKl} s_{Kl} \tag{3}$$

where σ_{iJ} and C_{iJKl} are the generalized stress and elasticity tensors. Using the contracted Voigt notation that reduces the fourth-order elastic and third order piezoelectric tensor to second order ones, these quantities and the generalized strain are given by

$$\sigma_{iJ} = \begin{pmatrix} \sigma_{11} \\ \sigma_{33} \\ \sigma_{13} \\ D_1 \\ D_3 \end{pmatrix}, s_{Kl} = \begin{pmatrix} s_{11} \\ s_{33} \\ 2s_{13} \\ -E_1 \\ -E_3 \end{pmatrix},$$

$$C_{iJKl} = \begin{pmatrix} c & e \\ e' & -\varepsilon \end{pmatrix}, c = \begin{pmatrix} c_{11} & c_{13} & 0 \\ c_{13} & c_{33} & 0 \\ 0 & 0 & c_{44} \end{pmatrix},$$

$$e = \begin{pmatrix} 0 & e_{31} \\ 0 & e_{33} \\ e_{15} & 0 \end{pmatrix}, \varepsilon = \begin{pmatrix} \varepsilon_{11} & 0 \\ 0 & \varepsilon_{33} \end{pmatrix} \tag{4}$$

Here $c_{11}, c_{33}, c_{44}, c_{13}$ are the elastic, $\varepsilon_{11}, \varepsilon_{33}$ are the dielectric and e_{31}, e_{33}, e_{15} are the piezoelectric constants. The elastic and dielectric constants are assumed to be positive definite, i.e. $c_{ijkl} q_{il} q_{kl} > 0, \quad \varepsilon_{jk} p_j p_k > 0$ for any real nonzero tensor q_{st} and vector p_s. These thermodynamically based conditions ensure a stable piezoelectric material. They express that the internal energy density must remain positive since this energy must be minimal in a state of equilibrium, see Dieulesaint & Royer (1974).

Assuming a time-harmonic motion with an angular frequency ω and suppressing the common term $e^{i\omega t}$, the balance equations (1) in generalized notation take the form

$$\sigma_{iJ,i} + \rho_{JK} \omega^2 u_K = 0 \tag{5}$$

where $\rho_{JK} = \begin{cases} \rho & J, K = 1, 3 \\ 0 & J = 4 \text{ or } K = 4 \end{cases}$. In what follows, traction-free crack faces $S_{cr} = S_{cr}^+ \cup S_{cr}^-$, i.e.

$$t_J = 0 \ \text{ on } \ S_{cr} \tag{6}$$

are supposed where $t_J = \sigma_{iJ} n_i$ is the generalized traction vector and n_i is the unit normal vector on S_{cr}^+. This specific boundary condition implies that the crack surfaces are free of both mechanical traction and surface charges, i.e. the crack is assumed to be electrically impermeable. In this case the electric field inside the crack is ignored and the crack may be thought as a low-capacitance medium with a potential drop $\Delta\Phi = \Phi^+ - \Phi^-$.

The interaction of an incident time-harmonic wave with the crack induces scattered waves. Due to the linearity of the problem the total wave field can be written as a sum of the incident and the scattered wave field:

$$u_J(x) = u_J^{in}(x) + u_J^{sc}(x), \quad t_J(x) = t_J^{in}(x) + t_J^{sc}(x) \tag{7}$$

The incident wave is assumed to be known while the scattered wave field is unknown. It has to satisfy the field equations (2)-(5), Sommerfeld's radiation condition at infinity and the boundary condition (6), which can be rewritten as

$$t_J^{sc} = -t_J^{in} \ \text{ on } \ S_{cr}^+ \tag{8}$$

Comparing the piezoelectric crack boundary value problem in generalized notation with that of the corresponding elastic problem, a total agreement can be stated, see e.g. Zhang & Gross (1998). In view of this, using the representation formulas, see Khutorianski & Sosa (1995a), Pan (1999) and Wang, Zhang & Hirose (2003) and following the procedure for the elastic case, the boundary value problem may be formulated in terms of a traction BIE in frequency domain. For the 2D case in plane strain it reads, see Gross, Dineva & Rangelov (2002) and Wang & Zhang (2004)

$$\begin{aligned} t_J^{in}(x) &= C_{iJKl} n_i(x) \\ &\int\limits_{S_{cr}^+} \Big[\Big(\sigma_{\eta PK}^*(x,y) \Delta u_{P,\eta}(y) - \rho_{QP} \omega^2 U_{QK}^*(x,y) \Delta u_P \Big) \delta_{\lambda l} \\ &\quad - \sigma_{\lambda PK}^*(x,y) \Delta u_{P,l}(y) \Big] n_\lambda dS_{cr} \ , \ x \in S_{cr}^+ \end{aligned} \tag{9}$$

where U_{QK}^* is the fundamental solution of Eq.(5) and $\sigma_{iJQ}^* = C_{iJKl} U_{KQ,l}^*$ are the corresponding stresses. Furthermore, $\Delta u_J = u_J|_{S_{cr}^+} - u_J|_{S_{cr}^-}$ is the unknown generalized crack opening displacement (COD) and δ_{ij} is the Kronecker symbol. Once the solution of (9), i.e. Δu_J, is known for a given frequency ω, the displacements and tractions of the scattered field and by this the total field in the whole region can be determined from the representations

$$u_J^{sc}(x) = -\int\limits_{S_{cr}^+} \sigma_{iMJ}^*(x,y) \Delta u_M(y) n_i(y) dS_{cr} \ , \ x \notin S_{cr}^+ \tag{10}$$

$$t_J^{sc}(x) = -C_{iJKl} n_i(x) \int\limits_{S_{cr}^+} \left[\left(\sigma^*_{\eta PK}(x,y) \Delta u_{P,\eta}(y) - \rho_{QP} \omega^2 U^*_{QK}(x,y) \Delta u_P \right) \delta_{\lambda l} - \sigma^*_{\lambda PK}(x,y) \Delta u_{P,l}(y) \right] n_\lambda dS_{cr} \ , \ x \notin S_{cr}^+ \tag{11}$$

3 Fundamental solution and incident plane wave

For the numerical solution of the integrodifferential equation (9), the traction t_J^{in} on the crack face due to the incident wave must be known. Furthermore, the fundamental solution U^* and the corresponding stress σ^* have to be available in an appropriate form. The derivation of the fundamental solution and the representation of the incident plane wave follow the lines given by Gross, Dineva & Rangelov (2002).

3.1 Fundamental solution

Since Eq. (5) has constant coefficients, a fundamental solution U^* exists, see John (1955), which can be represented as the 3×3 matrix $U^* = \{U^*_{KJ}\}$. Here U^*_{ij} and U^*_{4j} are the displacement in i-direction and the electric potential at a observation point $x = (x_1, x_3)$ due to an impulsive unit force applied at source point $x_0 = (x_{01}, x_{03})$ in j-direction while U^*_{i4} and U^*_{44} are the displacement in i-direction i and the electric potential on account of a unit point charge. As in the forgoing section, small subscripts vary by 1, 3 and capital subscripts by 1, 3, and 4. The matrix function U^* is solution of the equation

$$\left(D(\partial) + \rho\omega^2 J_3 \right) U^*(x, x_0) = -\delta(x - x_0) I_3 \tag{12}$$

where δ is the Dirac delta function, $J_q = \begin{pmatrix} I_{q-1} & 0 \\ 0 & 1 \end{pmatrix}$ with I_q Being the $q \times q$ unit matrix and the 3×3 matrix differential operator $D(\partial)$ consists on the elements $d_{JK}(\partial) = C_{iJKl} \partial_i \partial_l$.

The fundamental solution of the problem at hand can be derived by Radon transforms, see Ludwig (1966) and Zayed (1996). Let $f(x)$ be a function defined in R^2 and s be a real number, $m \in R^2$ then Radon transforms R of $f(x)$ is defined as

$$\hat{f}(s,m) = R[f(x)] = \int\limits_{<m,x>=s} f(x) d\Omega = \int\limits_{R^2} f(x).\delta(s - < m,x >) dx \tag{13}$$

where $<,>$ denotes the scalar product in R^2. This means, Radon transforms is an integration of $f(x)$ over all planes defined by $< m,x >= s$. The inverse Radon transform can be written as

$$f(x) = \frac{1}{4\pi^2} \int\limits_{|m|=1} K(\hat{f}(s,m))|_{s=<m,x>} dm,$$

$$K(\hat{f}) = \int\limits_{-\infty}^{+\infty} \frac{\partial_\sigma \hat{f}(\sigma, m)}{s - \sigma} d\sigma \tag{14}$$

The following Radon transforms properties will be used: $\hat{f}(\alpha s, \alpha m) = \frac{1}{\alpha} \hat{f}(s,m)$; $R(\alpha_1 f_1 + \alpha_2 f_2) = \alpha_1 \hat{f}_1 + \alpha_2 \hat{f}_2$; $R(\partial_j f(x)) = m_j \partial_s \hat{f}(s,m)$; $\quad R(\delta(x)) = \delta(s)$.

Applying Radon transforms to Eq. (12), taking for simplicity $x_0 = (0,0)$ and having in mind the Radon transform properties, we obtain

$$\left(D(m) \partial_s^2 + \rho\omega^2 J_3 \right) \hat{U}^*(s,m) = -\delta(s) I_3 \tag{15}$$

where the matrix $D(m)$ is obtained from $D(\partial)$ simply by replacing ∂_j by m_j. The matrix equation (15) consists of three systems with three linear equations. Expressing the functions $\partial_s^2 \hat{U}^*_{4J}$ by

$$\partial_s^2 \hat{U}^*_{4J} = d_{44}^{-1} \left(d_{k4} \partial_s^2 \hat{U}^*_{kJ} + \delta_{4J} \delta(s) \right) \tag{16}$$

it can be reduced to the matrix equation

$$\left(\tilde{D}(m) \partial_s^2 + \rho\omega^2 I_2 \right) \tilde{U}^*(s,m,\omega) = \tilde{F} \tag{17}$$

consisting of three systems with two equations where $\tilde{U}^*$ is a 2×3 matrix (the first two rows of $\hat{U}^*$). The so-called 'stiffened matrix' $\tilde{D}(m)$, see Daros (1999), is a 2×2 matrix with the components $\tilde{d}_{ij}(m) = d_{ij}(m) - d_{44}^{-1}(m) d_{i4}(m) d_{j4}(m)$ and $\tilde{F}$ is a 2×3 matrix with the components $\tilde{f}_{jK} = \delta_{jK} \delta(s) - d_{44}^{-1}(m) \delta_{4J} (\delta_{j1} + \delta_{j3}) \delta(s)$.

Equation (17) is a linear system of ordinary differential equations and in order to solve it, we will use its canonical form. On account of the properties of the material constants C_{iJKl}, the matrix $\tilde{D}(m)$ is symmetric and positive definite, i.e. $\left(Tr\tilde{D}(m) \right)^2 - 4 \det \tilde{D}(m) > 0$ is satisfied for every $m \neq 0$. Consequently, $\tilde{D}(m)$ has two different positive eigenvalues $b_1(m) > b_2(m) > 0$ and corresponding orthogonal and unit eigenvectors $g_1(m)$ and $g_2(m)$ exist. Their components form the orthogonal matrix $T(m) = \begin{pmatrix} g_1^1 & g_2^1 \\ g_1^2 & g_2^2 \end{pmatrix}$ that changes the basis to the

basis of eigenvectors. Substituting

$$\tilde{U}^*(s,m) = T(m)\,V(s,m) \quad ,$$
$$\tilde{F}(m,s) = T(m)F(m,s) \tag{18}$$

into Eq. (17), multiplying from the left side with $T^{-1}(m)$ and having in mind that

$$T^{-1}(m)\tilde{D}(m)T(m) = B(m) = \begin{pmatrix} b_1(m) & 0 \\ 0 & b_2(m) \end{pmatrix},$$

the system of equations (17) will be decoupled:

$$\left(B(m)\partial_s^2 + \rho\omega^2 I_2\right) V(s,m) = -F(s,m) \tag{19}$$

Equations (19) are six ordinary differential equations of the type

$$\left(b(m)\partial_s^2 + \rho\omega^2 I_2\right) \nu(s,m) = -\delta(s)\, f(m) \tag{20}$$

with the solution, see Vladimirov (1984),

$$\nu(s,m) = \alpha(m) f(s,m) e^{ik(m)|s|},$$
$$k(m) = \omega\sqrt{\rho/b(m)}, \alpha = i\,(2b(m)k(m))^{-1} \tag{21}$$

where $f(s,m)$ depends on g_j. Therefore, we get

$$\tilde{U}^* = TV, V_{pq} = \alpha_p g_q^p e^{ik_p|s|},$$
$$k_p = \omega\sqrt{\rho/b_p}, \quad \alpha_p = i\,(2b_p(m)k_p(m))^{-1} \tag{22}$$

Having $\tilde{U}^*_{kj} = \hat{U}^*_{kj}$ the function $\hat{U}^*_{4J}$ can be obtained from Eq. (16). From the 3×3 matrix $\hat{U}^*$ the fundamental solution U^* is constructed through inverse Radon transforms which is defined by Eq. (14).

Applying this procedure, the functions U^*_{ij}, $i,j = 1,3$ can be written as

$$\left\{U^*_{ij}(x,x_0)\right\} = \int\limits_{|m|=1} \begin{pmatrix} g_1^1 & g_2^1 \\ g_1^2 & g_2^2 \end{pmatrix} \begin{pmatrix} g_1^1 W_1 & g_1^2 W_1 \\ g_2^1 W_2 & g_2^2 W_2 \end{pmatrix} \Bigg|_{s=|\langle x-x_0,m\rangle|} dm \tag{23}$$

where

$$W_j(s) = B_j\Big[i\pi e^{ik_j s} - 2\big(ci\,(k_j s)\cos(k_j s) + si\,(k_j s)\sin(k_j s)\big)\Big], B_j = \left(8\pi^2 b_j\right)^{-1}$$

and

$$\mathrm{ci}\,(t) = -\int_t^\infty \frac{\cos(\tau)}{\tau} d\tau, \quad \mathrm{si}\,(t) = -\int_t^\infty \frac{\sin(\tau)}{\tau} d\tau$$

are the integral sin and integral cosine functions, see Bateman & Erdelyi (1953). The functions U^*_{i4} for $i = 1,3$ have the form

$$\left\{U^*_{i4}(x,x_0)\right\} = \int\limits_{|m|=1} \begin{pmatrix} g_1^1 & g_2^1 \\ g_1^2 & g_2^2 \end{pmatrix} \begin{pmatrix} g_4^1 W_1 \\ g_4^2 W_2 \end{pmatrix} \Bigg|_{s=|\langle x-x_0,m\rangle|} dm, \tag{24}$$

where $g_4^k = -d_{44}^{-1}\left(d_{14}g_k^1 + d_{34}g_k^2\right)$, $k = 1,2$ and finally

$$U^*_{44}(x,x_0) = h_1(x,x_0) + h_2(x,x_0), \tag{25}$$

where

$$h_1(x,x_0) = \Big\langle \int\limits_{|m|=1} \begin{pmatrix} g_1^1 & g_2^1 \\ g_1^2 & g_2^2 \end{pmatrix} \left(-d_{44}^{-1}\right) \begin{pmatrix} d_{14}g_4^1 W_1 \\ d_{34}g_4^2 W_2 \end{pmatrix} \Big|_{s=|\langle x-x_0,m\rangle|} dm, (1,1) \Big\rangle ,$$

$$h_2(x,x_0) = \frac{1}{4\pi^2} \int\limits_{|m|=1} d_{44}^{-1} \ln|s| \Bigg|_{s=|\langle x-x_0,m\rangle|} dm. \tag{26}$$

The derivatives of the fundamental solution U^* and its corresponding stress σ^* can be found using the function

$$\partial_s W_j(s) = B_j\Big[-\pi k_j e^{ik_j s} - \frac{2}{s} + 2k_j\big(ci\,(k_j s) \sin(k_j s) - si\,(k_j s)\cos(k_j s)\big)\Big]$$

Furthermore, from Eqs.(23)–(26) the near-field asymptotic of U^*_{IJ} and σ^*_{kIJ} yields as

$$U^*_{IJ} \approx b_{IJ} \ln|x - x_0|,$$
$$\sigma^*_{kIJ} \approx d_{kIJ} \frac{1}{|x-x_0|} \quad \text{for} \quad x \to x_0 \tag{27}$$

where b_{IJ} and d_{kIJ} depend on the elastic, dielectric and piezoelectric constants and the density, but not on the frequency ω. By comparison, it can be seen that the asymptotic behavior for the time-harmonic case is the same as for the corresponding static case, see Rajapakse & Xu (2001). It also shall be mentioned that the fundamental solutions for the elastic-isotropic and elastic-anisotropic cases can also be derived by following the procedure described above. Note that for the anisotropic case the transient and time-harmonic fundamental solution has been obtained by Wang & Achenbach (1994).

3.2 Incident plane wave

The incident wave displacement u_J^{in} and traction t_J^{in} are obtained as solution of Eq. (5) using the wave decomposition method, see Courant & Hilbert (1962). At a fixed frequency ω we seek a solution in form of a plane wave

$$\overline{U}(x,\xi) = p.\exp\left\{-i\overline{k}\,\langle x,\xi\rangle\right\} \tag{28}$$

where $\xi = (\xi_1, \xi_3)$ is a given wave propagation direction and the polarization vector $p = (p_1, p_3, p_4)$ and the real wave number $\overline{k}$ are unknown. The vector function $\overline{U}$ has to satisfy Eq. (12) with zero right hand side:

$$\left(D(\partial) + \rho\omega^2 J_3\right)\overline{U}(x,\xi) = 0 \tag{29}$$

Applying the procedure described in section 3.1, the generalized plane wave solution is found as a superposition of the two types of incident plane waves

$$\begin{aligned}&\overline{U}^j(x,\xi) = p^j \exp\left\{-i\overline{k}_j\,\langle x,\xi\rangle\right\},\\ &\overline{k}_j = \omega\sqrt{\rho/\beta_j(\xi)}, \quad j = 1,2\end{aligned} \tag{30}$$

where $\beta_j > 0$ are the eigenvalues of the stiffened matrix $\tilde{D}(\xi)$, $\tilde{p}^j = (p_1^j, p_3^j)$ are the unit and orthogonal eigenvectors of $\tilde{D}(\xi)$ and $p_j^4 = -d_{44}^{-1}(\xi) d_{i4} p_i^j$.

The linear combination $\overline{U} = \alpha_1\overline{U}^1 + \alpha_2\overline{U}^2$ represents the set of all plane wave solutions of Eq. (5) where $\alpha_1 = 1, \alpha_2 = 0$ corresponds to L-waves, while $\alpha_1 = 0, \alpha_2 = 1$ corresponds to SV-waves. Note that in contrast to isotropic elasticity the eigenvalues β_1, β_2 depend in anisotropic and piezoelectric cases on the wave propagation direction ξ. Using Eqs. (2) – (4) the generalized incident stress tensor and corresponding traction vector on the crack S_{cr}^+ that appears on the left hand side of Eq. (9) can be determined.

For example, let the crack S_{cr}^+ be a segment on the x_1-axis and let the incident wave be a L-wave with incidence angle $\theta = \pi/2$, i.e. normal to the crack, then the expression for the incident displacement field has the form, see Eq. (30), $\overline{u}_1^{in} = 0$, $\overline{u}_3^{in} = e^{-i\overline{k}_1 x_3}$, $\overline{u}_4^{in} = e_{33}\varepsilon_{33}^{-1} e^{-i\overline{k}_1 x_3}$ where $\overline{k}_1 = \omega\sqrt{\left(c_{33} + e_{33}^2\varepsilon_{33}^{-1}\right)^{-1}\rho}$ and the incident traction on the crack is

$$\overline{t}_1^{in} = 0\,,\ \overline{t}_3^{in} = -i\omega\sqrt{\left(c_{33} + e_{33}^2\varepsilon_{33}^{-1}\right)\rho}\,,\ \overline{t}_4^{in} = 0\,. \tag{31}$$

4 Numerical solution procedure

The numerical solution scheme follows that developed in Dineva, Gross & Rangelov (1999, 2002) and Rangelov, Dineva & Gross (2003) for an isotropic material. The non-hypersingular traction BIEs are collocated on one side of the crack boundary using displacement jumps (COD) as unknowns. The displacement and traction are approximated with parabolic shape functions which satisfy Hölder continuity at least at the collocation points and show an asymptotic $O(\sqrt{r})$-COD behaviour near the crack tips. Quarter-point boundary elements (QP-BE) are implemented in a quadratic boundary element discretization. The disadvantage of the standard quadratic approximation regarding the smoothness at all irregular points is overcome by the shifted point method. After discretization the obtained integrals are at least CPV integrals. The regular integrals are computed employing the Gaussian quadrature scheme for one-dimensional integrals and Monte Carlo integration scheme for two-dimensional integrals. All integrals with singular kernels are solved analytically in the small neighbourhood of the field point, using the approximation of the fundamental solution for a small argument.

After discretization of the non-hypersingular traction BIEs (9) and satisfying boundary conditions on the crack, an algebraic system of equations for the CODs is obtained and solved. The SIFs directly are obtained from the traction nodal values ahead of the crack tip, see Aliabadi & Rooke (1991), Suo, Kuo, Barnett & Willis (1992).

The program codes basing on Mathematica and FORTRAN have been created following the above described procedure.

5 Validation and numerical results

In order to validate the described approach, a straight crack in a transversely-isotropic piezoelectric plane under normal incident L-waves is investigated. The results for the stress intensity factors are compared with those of Shindo & Ozawa (1990), who reduced this problem by Fourier transforms to a pair of dual integral equations and finally expressed its solution in terms of a Fredholm integral equation of second kind. Subsequently, to study the dependence of the stress intensity factors on the different parameters, results are presented for L- and SV-wave loading, for different angles of incidence and for

different material constants.

In all numerical examples, the crack of length $2a$ is located in the interval$(-a,+a)$ on the x_1-axis. It is divided into 7 boundary elements and the shifted points numerical scheme is used. The generalized dynamic SIF's are calculated by using the formulae

$$\begin{aligned} K_I &= \lim_{x_1\to a^{\pm}} t_3\sqrt{2\pi(x_1\mp a)}\,, \\ K_{II} &= \lim_{x_1\to a^{\pm}} t_1\sqrt{2\pi(x_1\mp a)}\,, \\ K_{IV} &= \lim_{x_1\to a^{\pm}} t_4\sqrt{2\pi(x_1\mp a)} \end{aligned} \tag{32}$$

where t_J is the generalized traction at the point $(x_1,0,0)$ close to the crack-tip. For convenience they are normalized by an appropriate static value, i.e. the normalization coefficient for the mechanical SIF's is

$$\begin{aligned} k &= \overline{k}_1(\xi,\omega)b_1(\xi,\omega)\big|_{\xi=(0,1)}\sqrt{\pi a} = \left|\overline{t}_3^{in}\right|\sqrt{\pi a} \\ &= \omega\left[\left(c_{33}+e_{33}^2\varepsilon_{33}^{-1}\right)\rho\right]^{1/2}\sqrt{\pi a} \end{aligned} \tag{33}$$

where $\overline{t}_3^{in}$ is the traction of the normal incident L wave given by Eq. (31). The generalized displacement u_I^{in} and generalized traction $t_J^{in}=\sigma_{iJ}^{in}n_i$ for an incidence angle θ and at the point $x=(x_1,0,0)\in S_{cr}$ are obtained from Eq. (30), where $\overline{U}^1$, $\overline{U}^2$ are used for the L and SV-wave respectively.

The materials constants of the three different piezoelectric materials under consideration are taken from Dieulesaint & Royer (1974) and listed in Tab. 1. For the validation test and the study of the dependence on the wave incidence angle PZT-6B is used.

Figs. 2a,b show the variation of the normalized mechanical mode I and the normalized electrical field stress intensity factor $\left|e_{33}k^{-1}K_E\right|$ versus the normalized frequency $\Omega=a\omega\sqrt{\rho c_{44}^{-1}}$. Note that in the case of a normal incident L-wave, according to Eq. (30), $E_1=0$ and $u_1=0$ holds and E_3 can be obtained at every point along x_1 out of the crack from the constitutive equation (3), i.e.

$$\left|\begin{array}{l} t_3 = c_{33}u_{3,3}-e_{33}E_3 \\ t_4 = e_{33}u_{3,3}+\varepsilon_{33}E_3 \end{array}\right. \tag{34}$$

from which

$$E_3=(t_4c_{33}-e_{33}t_3)\left(\varepsilon_{33}c_{33}+e_{33}^2\right)^{-1} \tag{35}$$

Then $K_E=\lim_{x\to a^{\pm}} E_3\sqrt{2\pi\,(x\mp a)}$ where the electric field E_3 is calculated from (35) at a point close to the crack-tip.

Table 1 : Properties of the piezoelectric materials.

Constants		PZT-5H	PZT-6B	PZT-7A
Elastic stiffness $10^{10}\,N/m^2$	c_{11}	12,6	16,8	14,8
	c_{13}	5,3	6,0	7,42
	c_{33}	11,7	16,3	13,1
	c_{44}	3,53	2,71	2,54
Piesoelectric coefficients C/m^2	e_{31}	-6,5	-0,9	-2,1
	e_{33}	23,3	7,1	9,5
	e_{15}	17,0	4,6	9,7
Dielectric constants $10^{-10}\,C/Vm$	ε_{11}	151	36	81,1
	ε_{33}	130	34	73,5
Density $10^3\,kg/m^3$	ρ	7,6	7,55	7,5

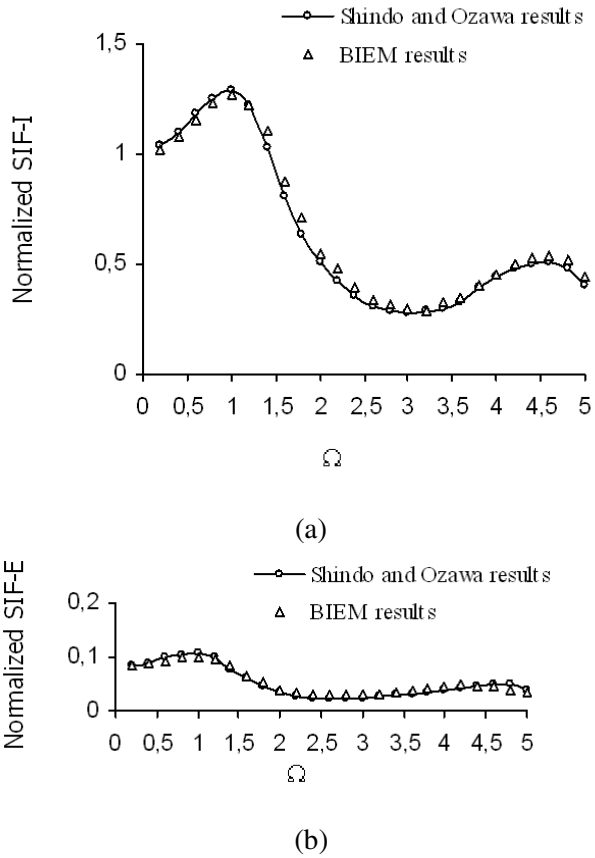

Figure 2 : Dynamic SIF versus frequency Ω for normal incident L wave: a) mechanical SIF-I, b) electrical SIF-E

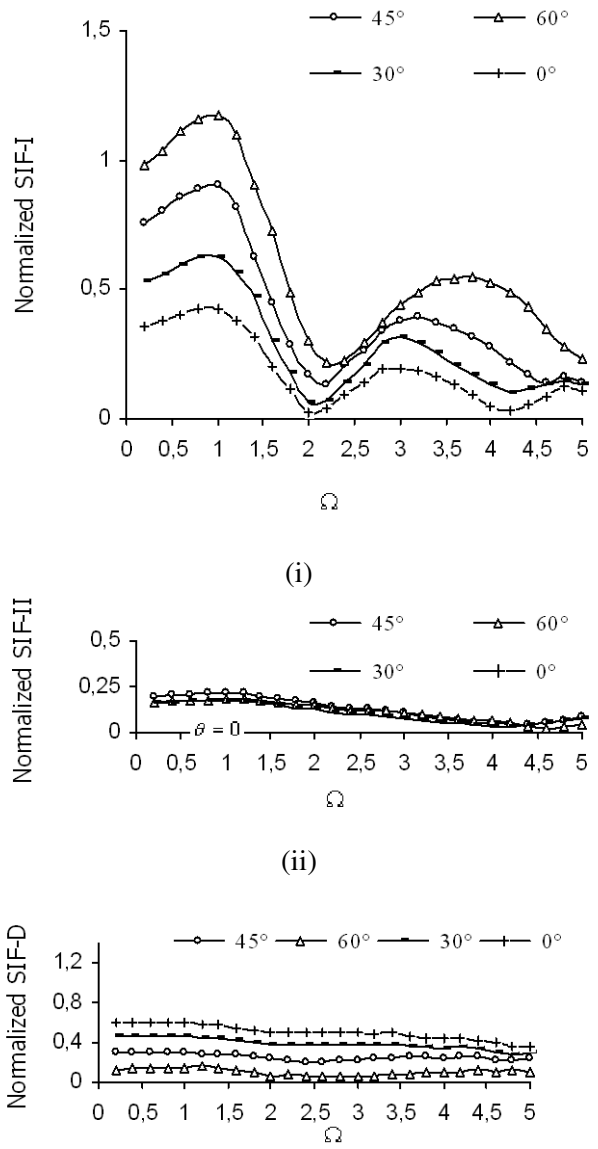

Figure 3a : Dynamic SIFs versus frequency Ω for L-wave loading with different incidence angle: (i) mechanical SIF-I, (ii) mechanical SIF-II, (iii) electrical SIF-D.

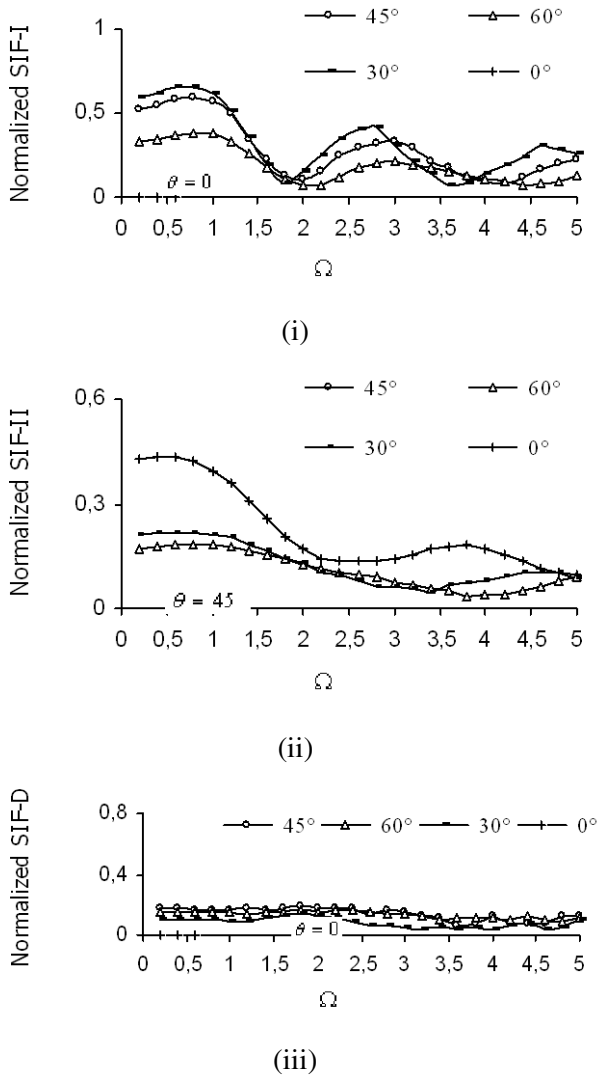

Figure 3b : Dynamic SIFs versus frequency Ω for SV-wave loading with different incidence angle: (i) mechanical SIF-I, (ii) mechanical SIF-II, (iii) electrical SIF.

Figs. 2a, b show a very good agreement between the results of Shindo and Ozawa (1990) and the used BIEM technique. The maximum differences within the considered frequency domain are 7-8 %. This approves the accuracy and applicability of the non-hypersingular traction based BIEM for the solution of 2D in-plane wave problems in piezoelectric materials with cracks.

In the following, a set of numerical results for a wave loaded straight crack is presented highlighting the dependence of the stress intensity factors on the frequency, the wave type, the incidence angle and the material constants. Note that in Figs. 2 and 4 (for the incidence angle $\theta = \pi/2$) the normalized mechanical and electric field intensity factor $\left|e_{33}k^{-1}K_E\right|$ are displayed while in Figs. 3, 5 and 6 the normalized mechanical and electric displacement intensity factor $\left|c_{33}(e_{33}k)^{-1}K_D\right|$ are depicted.

Figs. 3a,b display for incident L and SV-waves the dynamic normalized SIFs versus normalized frequency Ω for different angles of incidence.

The first maximum of the SIF-I for an incident L-wave,

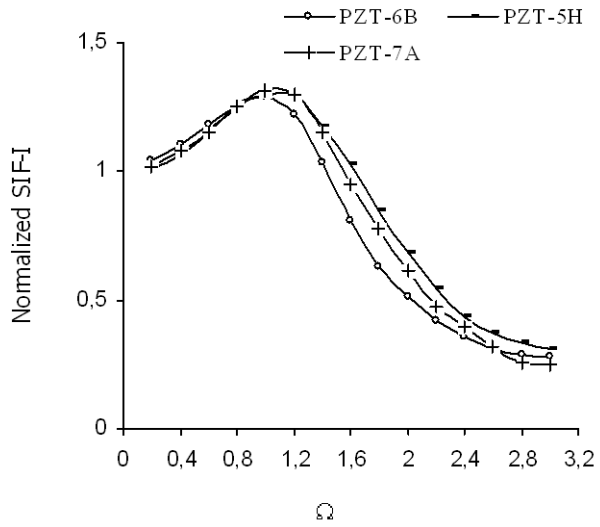

(i)

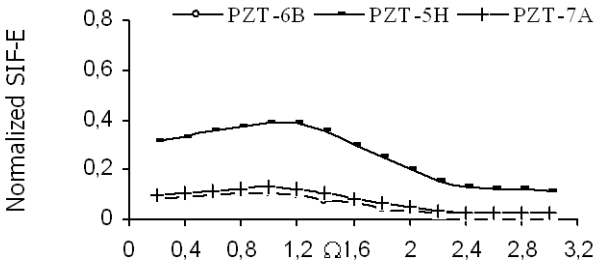

(ii)

Figure 4a : Dynamic SIF versus frequency Ω for normal incident L waves and three different materials: (i) mechanical SIF-I, (ii) electrical SIF-E.

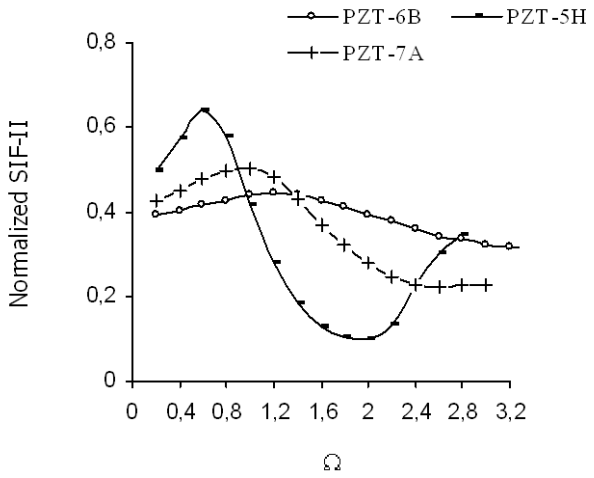

Figure 4b : Dynamic SIF-II versus frequency Ω for normal incident SV waves and three different materials

see Fig. 3a (i), appears approximately at $\Omega = 1$ for all considered angles of incidence. Its amplitude, commonly called dynamic amplification, decreases from 1,289 for $\theta = 90^0$ and 1.173 for $\theta = 60^0$ to 0.429 for $\theta = 0^0$ (grazing incidence). The second peak occurs at different frequencies depending on the incidence angle. The SIF-II curves in Fig. 3a (ii) indicate close results for L-wave incidence angles 30^0, 45^0 and 60^0, except $\theta = 0^0$ where SIF-II is zero. The electrical displacement SIF-D in Fig. 3a (iii) has its maximal values for an incidence angle $\theta = 0^0$ and minimal ones for $\theta = 60^0$. The dependence on the frequency is weak.

The first maximum of SIF-I in case of an incident SV-wave, see Fig. 3b (i), appears approximately at $\Omega = 0.8$ for all considered angles of incidence. The dynamic amplification varies here from 0.6592 for $\theta = 30^0$, 0.589 for $\theta = 45^0$ to 0.383 for $\theta = 60^0$. The second peak again occurs at different frequencies depending on the wave incidence angle. The SIF-II curves in Fig. 3b (ii) show maximal values for SV-waves at an incidence angle $\theta = 0^0$ while at $\theta = 45^0$ SIF-II is zero. The electrical displacement SIF-D in Fig. 3b (iii) again is weakly dependent on the frequency and displays close results for incidence angles 30^0, 45^0 and 60^0; at $\theta = 0^0$ SIF-D is zero.

The sensitivity of the stress intensity factors to the material parameters can be seen from Fig. 4a,b. It shows the normalized SIF's versus normalized frequency Ω for normal incident L and SV-waves and three different piezoelectric materials. For L-wave loading it can be seen from Fig. 4a that PZT-5H delivers the highest SIF values followed by PZT-6B. The SIF curves for PZT-7A is in between the SIF curves for PZT-5H and PZT-6B. While the dependence of SIF-I on the material is relatively weak this cannot be said for SIF-E. For SV-wave loading a strong dependence of SIF-II on the material constants can be observed from Fig. 4b. PZT-5H again delivers the maximum dynamic amplification followed by PZT-7A.

The influence of the wave type, the incidence angle and the material constants on the amplification effect is depicted in Figs. 5 and 6 where the normalized SIFs versus incidence angle at fixed frequency $\Omega = 0.8$ are displayed for L and SV-waves and three different piezoelectric ceramics. The SIF-I and II dependence on the angle of in-

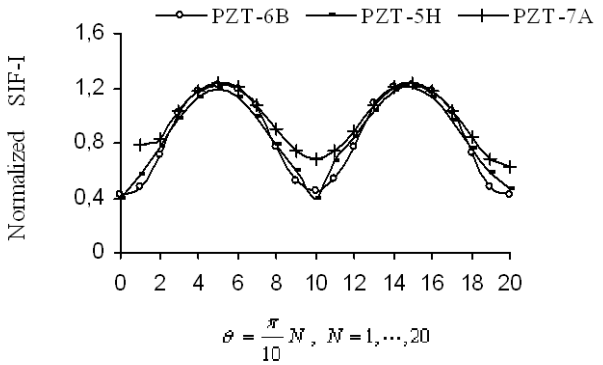

(i)

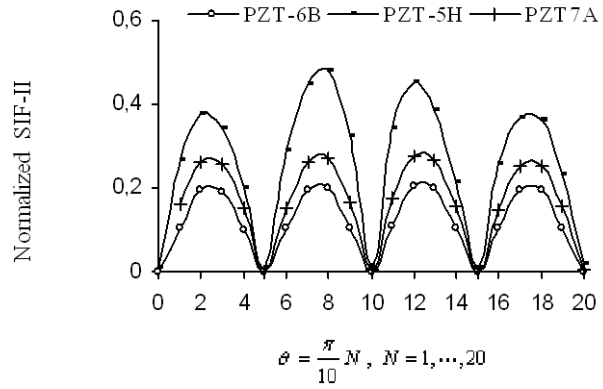

(ii)

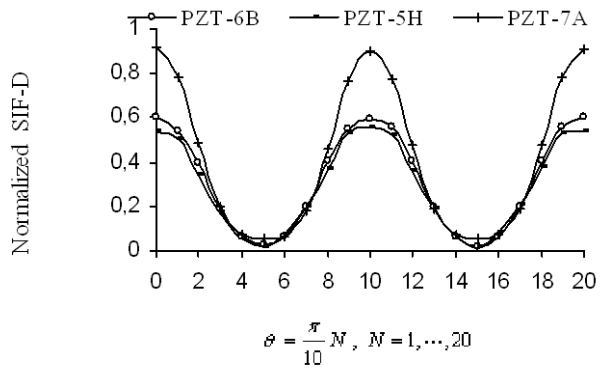

(iii)

Figure 5 : Dynamic SIF versus incidence angle for L-wave loading at fixed frequency $\Omega = 0.8$ for three different materials: (i) mechanical SIF-I, (ii) mechanical SIF-II, (iii) electrical SIF.

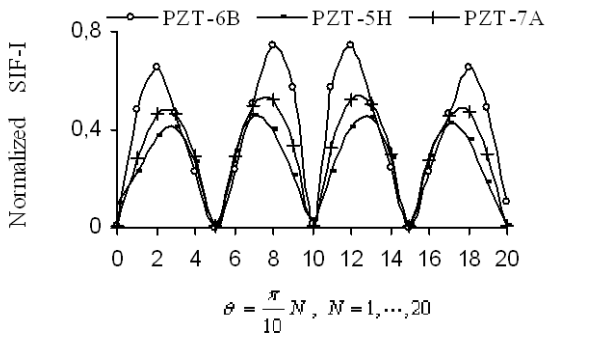

(i)

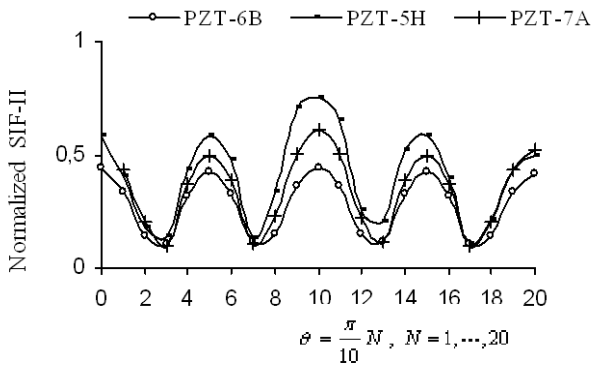

(ii)

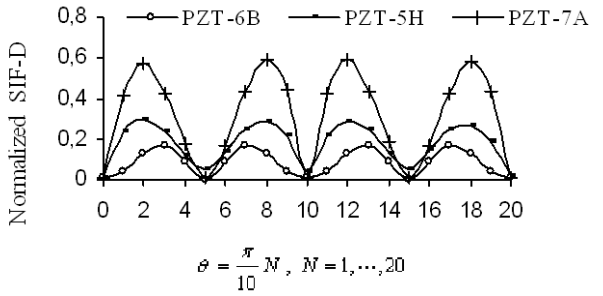

(iii)

Figure 6 : Dynamic SIF versus incidence angle for SV-wave loading at fixed frequency $\Omega = 0.8$ for three different materials: (i) mechanical SIF-I, (ii) mechanical SIF-II, (iii) electrical SIF

cidence and on the type of the incident wave are qualitatively similar to corresponding curves presented in Sih (1977) for a crack in an elastic isotropic medium. The electrical displacement intensity factors for both wave types are depicted in Fig. 5 (iii) and Fig. 6 (iii).

Generally, the study shows that the dynamic mechanical and electrical SIF's are quite sensitive to the type of the wave, the frequency, the angle of incidence and also to

the piezoelectric material properties.

6 Conclusion

A 2D analysis of an arbitrarily shaped crack in an infinite transversely isotropic piezoelectric material is presented by non-hypersingular traction BIEM in frequency domain. The 2D dynamic fundamental solution obtained by Radon transform in frequency domain is derived in closed form. A numerical scheme for the solution and determination of generalized SIF's is validated by comparison with results for the line crack from the literature. It shows a good accuracy even when the crack is discretized by a low number of elements.

Parametric studies for the diffraction of longitudinal and shear waves by the line crack under different angles of incidence, at different frequencies and for different piezoelectric materials are presented. The results show that the stress intensity factors strongly depend on the combined influence of the aforementioned parameters.

The derived fundamental solution, the numerical scheme presented and the program codes developed can be used as a good basis for the solution of dynamic piezoelectric problems with a more complex geometry (e.g. finite cracked multilayered regions) and mechanics (e.g. general anisotropy, crack-interaction, inhomogeneity), different dynamic loading (e.g. transient) and different type of the electrical boundary conditions.

Acknowledgement: The authors acknowledge the support of the DFG under the grant number 436BUL 113/118/0-1.

7 References

Aliabadi, M.; D. Rooke. (1991): *Numerical fracture mechanics.* Computation Mechanics Publications, Southampton.

Bateman, H.; Erdelyi, A. (1953): *Higher transcendental functions,* McGraw-Hill, New York.

Benjeddou, A. (2000): Advances in piezoelectric finite element modeling of adaptive structural elements: a survey. *Computers and Structures,* vol.76 (1-3), pp. 347-363.

Chen, T.; Lin, F.Z. (1995): Boundary integral formulations for three-dimensional anisotropic piezoelectric solids. *Computational Mechanics,* vol.15 (6), pp. 485-496.

Chen, Z.T.; Yu, S. (1998): Anti-plane vibration of cracked piezoelectric materials. *Mechanics Research Communications,* vol. 25(3), pp. 321-327.

Courant, R.; Hilbert, D. (1962): *Methods of Mathematical Physics*, vol. II, Wiley, New York.

Daros, C.H. (1999).Wave propagation in unbounded piezoelectric media of transfersely isotropic symmetry. *Ph.D. dissertation, Series on Mechanics,* No. 39, Braunschweig.

Daros, C.H. (2002): A fundamental solutions for transversely isotropic, piezoelectric solids under electrically irrotational approximation. *Mechanics Research Communications,* vol. 29, pp. 61-71.

Daros, C. H.; Antes, H. (2000) : Dynamic fundamental solutions for transversely isotropic piezoelectric materials of crystal class 6mm. *International Journal of Solids and Structures,* vol. 37, pp.1639-1658.

Davi, G.; Milazzo, A. (2001): Multidomain boundary integral formulation for piezoelectric materials fracture mechanics. *International Journal of Solids and Structures,* vol. 38, pp. 7065-7078.

Denda, M.; Lua, J. (1999): Development of the boundary element method for 2D piezoelectricity. *Composites: PartB,* vol. 30, pp. 699-707.

Denda, M.; Araki, Y.; Yong, Y.K. (2004): Time – harmonic BEM for 2-D piezoelectricity applied to eigenvalue problems. *International Journal of Solids and Structures,* vol. 41, pp. 7241-7265.

Dieulesaint, E.; Royer, D. (1974): *Elastic wave in Solids.* John Wiley, New York.

Dineva, P.; Gross, D.; Rangelov, T. (1999): Ultrasonic wave scattering by a line crack in a solder joint. *Research Nondestructive Evaluation,* vol. 11, pp. 117-135.

Dineva, P.; Gross, D.; Rangelov, T. (2002): Dynamic behaviour of a cracked solder joint. *Journal of Sound and Vibration,* vol. 256(1), pp. 81-102.

Eringen, A.C.; Maugin, G.A. (1990): *Electrodynamics of Continua I: Foundations and Solid Media*, Springer Verlag, Berlin.

Gross, D.; Dineva, P.; Rangelov, T. (2002): Dynamic fracture behaviour of a multilayered piezoelectric solid. *Research reports*, DFG grant 436 BUL 113/118-1, TU Darmstadt.

Gross, D.; Dineva, P.; Rangelov, T. (2004): BIEM for cracked piezoelectric solids under dynamic load. In: Z.H. Yao; M.W. Yuan; W.X. Zhong, (Eds.), *Proceedings of the WCCM VI in conjuction with APCOM'04* September 5-10, Tsingua University Press& Springer Verlag, Beijing, China.

Hill, L.R.; Farris, T.N. (1998): Three-dimensional piezoelectric boundary element method. *AIAA Journal,* vol. 36(1), pp. 102-108.

Ikeda, T. (1990): *Fundamentals of Piezoelectricity,* Oxford University Press,

John, F. (1955): *Plane waves and spherical means applied to partial differential equations*, Interscience, New York.

Khutoryansky, N.M.; Sosa, H., (1995a): Dynamic representation formulas and fundamental solutions for piezoelectricity. *International Journal of Solids and Structures,* vol. 32,pp. 3307-3325.

Khutoryansky, N.M.; Sosa, H., (1995b): Construction of dynamic fundamental solutions for piezoelectric solids. *Appl. Mech. Review,* vol. 48 (11), pp. 222-229.

Kumar, S.; Singh, R.N. (1997a): Energy release rate and crack propagation in piezoelectric materials. Part I: mechanical/electrical load. *Acta Mater,* vol. 45, pp. 849-857.

Kumar, S.; Singh, R.N. (1997b): Energy release rate and crack propagation in piezoelectric materials. Part II: combined mechanical and electrical load. *Acta Mater,* vol. 45, pp. 859-868.

Landau, L.D.; Lifshitz, E.M. (1960): *Electrodynamics of Continuous Media.* Pergamon Press, Oxford.

Lee J. S., (1999): Boundary element method for electroelastic interaction in piezoceramics. *Engineering Analysis with BE,* vol. 15, pp. 321-328.

Ludwig, D. (1966): The Radon Transform on Euclidean Space. *Comm. Pure Appl. Math,* vol. 29, pp. 49-81.

McMeeking, R.M. (1999): Crack tip energy release rate for a piezoelectric compact tension specimen. *Engineering Fracture Mechanics,* vol. 64, pp. 217-244.

Narita, F.; Shindo, Y. (1998): Dynamic anti-plane shear of a cracked piezoelectric ceramic. *Theoretical and Applied Mechanics,* vol. 29, pp. 169-180.

Norris, A.N. (1994): Dynamic Green's functions in anisotropic piezoelectric, thermoelastic and poroelastic solids. *Proceedings of the Royal Society of London,* vol. *A*447,pp. 175-188.

Pak, Y.E. (1990): Crack extension force in a piezoelectric material. *J. Appl. Mech,*vol. 57,pp. 647-653.

Pan, E. (1999): A BEM analysis of fracture mechanics in 2D anisotropic piezoelectric solids. *Engineering Analysis with BE,* vol. 23, pp. 67-76.

Parton, V.Z. (1976): Fracture mechanics of piezoelectric materials. *Acta Astronautica,* vol. 3 (9-10), pp. 671-683.

Parton V.Z.;Kudryavtsev, B.A. (1988): *Electromagnetoelasticity.* Gordon and Breach Science Publishers,New York.

Rajapakse, R.K.N.D.; Xu X.-L. (2001): Boundary element modelling of cracks in piezoelectric solids. *Engineering Analysis with BE,* vol. 25, pp. 771-781.

Rangelov, T.; Dineva, P. (2004): Scattering from the line crack in piezoelectric solid. *C. R. Acad. Sci. Bulg.vol.* 57(3), pp. 17-22.

Rangelov, T.; Dineva, P.; Gross, D. (2003): A hypersingular traction boundary integral equation method for stress intensity factor computation in a finite cracked body. *Engineering Analysis with BE,* vol. 27, pp. 9-21.

Ray, M.C.; Bhattacharya, B.; Samanta, B. (1998):. Exact solutions for dynamic analysis of composite plates with distributed piezoelectric layers. *Computers and Structures,* vol. 66(6), pp. 737-743.

Saez, A.; Dominguez, J.; Garcia-Sanchez, F. (2004): BEM for cracked piezoelectric solids. In: Z.H. Yao; M.W. Yuan; W.X. Zhong, (Eds.), *Proceedings of the WCCM VI in conjuction with APCOM'04* September 5-10, Tsingua University Press & Springer Verlag, Beijing, China.

Sih, G.C. (1977): *Mechanics of fracture 4, Elastodynamic crack problems* , Noordhoff International Publishing, Leyden, The Netherlands.

Shang, F.; Kuna, M.; Abendroth, M. (2003): Finite element analysis of three-dimensional crack problems in piezoelectric structures. *Engineering Fracture Mechanics,* vol.70,pp. 143 – 160.

Shindo, Y.; Ozawa, E. (1990): Dynamic analysis of a cracked piezoelectric material. In: R.K.T. Hsieh, (Ed.), *Mechanical Modeling of New Electromagnetic materials.* Elsevier, Amsterdam, pp. 297-304.

Shindo, Y.; Katsura, H.; Yan, W. (1996): Dynamic stress intensity factor of a cracked dielectric medium in a

uniform electric field. *Acta Mechanica,* vol.117,pp.1-10.

Sosa, H. (1992): On the fracture mechanics of piezoelectric solids. *International Journal of Solids and Structures,* vol. 29,pp. 2613-2622.

Sosa, H.; Khutoryansky, N. (1999): Transient dynamic response of piezoelectric bodies subjected to internal electric impulses. *International Journal of Solids and Structures,* vol. 36, pp. 5467-5484

Sosa, H.; Khutoryansky, N. (2001): Further analysis of the transient dynamic response of piezoelectric bodies subjected to electric impulses. *International Journal of Solids and Structures,* vol. 38, pp. 2101-2114.

Suo, Z.; Kuo, C.-M.; Barnett, D.M.; Willis, J.R. (1992): Fracture mechanics for piezoelectric ceramics. *J. Mech. Phys. Solids,* vol. 40, pp. 739-765.

Vladimirov, V. (1984): *Equations of mathematical physics*, Nauka, Moskow.

Wang, B.L.; Noda, N. (2000): A cracked piezoelectric material under generalized plane electromechanical impact. *Arch. Mech,* vol. 52(6), pp. 933-948.

Wang, C.-Y.; Achenbach, J. (1994): Elastodynamic fundamental solutions for anisotropic solids, *Geophysics Journal International*, vol. 118, pp. 384-392.

Wang, C.-Y.; Zhang C. (2004): 2D and 3D dynamic Green's functions and time-domain BIE formulations for piezoelectric solids, In: Z.H. Yao; M.W. Yuan; W.X. Zhong, (Eds.), *Proceedings of the WCCM VI in conjuction with APCOM'04* September 5-10, Tsingua University Press& Springer Verlag, Beijing, China.

Wang, C.-Y.; Zhang, CH.; Hirose, S. (2003): Dynamic fundamental solutions and time domain BIE formulations for piezoelectric solids, In: R. Gallego, M.H. Aliabadi,(Eds.), *Advances in Boundary Element Techniques IV*, Queen Mary and Westfield College, University of London, pp. 215-225.

Wang, X.D.; Meguid, S.A. (2000a): Effect of electromechanical coupling on the dynamic interaction of cracks in piezoelectric materials. *Acta Mechanica,* vol. 143,pp. 1-15.

Wang, X.D.; Meguid, S.A. (2000b): Modelling and analysis of the dynamic behavior of piezoelectric materials containing interacting cracks. *Mechanics of Materials,* vol. 32, pp. 723-737.

Xu, X.-L. ; Rajapakse, R.K.N.D. (1998): Boundary element analysis of piezoelectric solids with defects. *Composites:Part* , vol. 29B, pp. 655-669.

Zayed, A. (1996): *Handbook of Generalized Function Transformations*, CRC Press, Boca Raton, Florida.

Zhang, C.; Gross, D. (1998): *On wave propagation in elastic solids with crac*ks.Computational Mechanics Publications, Southampton.

Zhao, X.; Meguid, S.A. (2002): On the dynamic behaviour of a piezoelectric laminate with multiple interfacial collinear cracks. *International Journal of Solids and Structures,* vol. 39, pp. 2477-2494.